Spin-glass behavior in hexagonal $Na_{0.70}MnO_2$

L. B. Luo, Y. G. Zhao,* G. M. Zhang, and S. M. Guo
Department of Physics, Tsinghua University, Beijing 100084, China

Z. Li and J. L. Luo
Beijing National Laboratory for Condensed Matter Physics, Institute of Physics, Chinese Academy of Sciences, Beijing 100080, China

(Received 13 October 2006; revised manuscript received 2 February 2007; published 23 March 2007)

In this paper, we present an experimental study of the hexagonal compound $Na_{0.70}MnO_2$. Zero-field-cooled and field-cooled susceptibilities display divergences at low temperatures, and the magnetic measurements of frequency dependence of ac susceptibility, hysteresis effect, and long-time relaxation are performed, indicating that $Na_{0.70}MnO_2$ undergoes a spin-glass transition at $T_f=39$ K. The spin-glass order parameter $q(T)$ determined from the dc spin susceptibility exhibits the relation $q(T)\propto(1-T/T_f)$, in agreement with the prediction of conventional spin-glass theory. Spin dynamics in the spin-glass state is carefully examined, and the time decay of the thermoremanent magnetization can be well scaled with a reduced effective waiting time λ/t_w^{μ}. The magnetic entropy extracted from the specific heat implies that the spin degrees of freedom of Mn^{3+}/Mn^{4+} ions are completely frozen at low temperatures, and the origin of this spin-glass behavior is attributed to the mixture of Mn^{3+}/Mn^{4+} ions and geometrical frustrations on the triangular lattices. Comparisons with the magnetic properties of $Na_{0.70}CoO_2$ are also made.

DOI: 10.1103/PhysRevB.75.125115 PACS number(s): 71.27.+a, 75.50.Lk, 75.47.Lx

INTRODUCTION

In the last two decades, triangular lattice antiferromagnets have attracted considerable attentions due to their rich quantum phenomena.[1] The triangular arrangements of magnetic moments with each pair coupled antiferromagnetically tend to hinder the system to find a unique ground state, i.e., the geometrical frustration.[2] Among them, Na_xCoO_2 has enjoyed intense studies in recent years. Superconductivity with transition temperature $T_c\approx 4$ K was observed in the hydrated compound $Na_xCoO_2\cdot yH_2O$ ($x\approx 0.30$, $y\approx 1.3$),[3] while large thermopower and low electrical resistivity coexist in the unhydrated compound Na_xCoO_2 for $x\approx 0.7$.[4,5] Unexpectedly, an insulating state at $x=0.50$ was observed, involving charge ordering and Na superstructure lattice.[6] The interactions of sodium ions with the underlying cobalt lattice in both hydrated and unhydrated Na_xCoO_2 give rise to a wide range of possible structure-property relationship.[6,7] The consequences of strong Coulomb repulsion with geometrical frustration are being intensively investigated.

Experiments have shown large electron-electron scattering[8] and strong spin fluctuation in $Na_{0.70}CoO_2$,[9,10] and a possible proximity to the quantum critical point was also suggested.[11] In our previous paper, singular electronic transports and magnetic and thermodynamic properties have been observed in Mn-doped $Na_{0.70}CoO_2$, revealing enhanced magnetic fluctuation and possible quantum critical behavior.[12] These results make us think about the manganese doping extreme $Na_{0.70}MnO_2$ compound, where all the cobalt ions are replaced by the manganese ions. It is fundamentally interesting to study the magnetotransport properties of $Na_{0.70}MnO_2$ and how the spin degrees of manganese ions of this compound acclimatize themselves to the geometrical frustrations. Fortunately, hexagonal $Na_{0.70}MnO_2$ has the analogous structure with $Na_{0.70}CoO_2$, offering a good opportunity to have a comparison between them. The synthesis and structure studies of $Na_{0.70}MnO_2$ had been fully performed;[13,14] however, the detailed magnetic measurements are still lacking. In addition, recent experiments have reported the complex ground state in some kindred compounds Na_xMO_2 (M=Ni, Cr).[15–17] So experimental investigations of the hexagonal compound $Na_{0.70}MnO_2$ will shed light on the understanding of the family compounds of sodium transition-metal oxides.

In this paper, detailed measurements of magnetic and thermodynamic properties in the hexagonal compound $Na_{0.70}MnO_2$ are performed. It is found that canonical spin-glass transition is displayed at low temperatures. The properties of this spin-glass state (including irreversibility, hysteresis effect, long-time relaxation, magnetic entropy, and order parameter) are obtained. The origin of the spin-glass behavior is carefully analyzed, and a comparison with the magnetic properties of $Na_{0.70}CoO_2$ is addressed.

EXPERIMENT

Polycrystalline samples with nominal composition $Na_{0.70}MnO_2$ were prepared by the solid-state reaction method. The detailed preparation procedure can be found in the published work of Paulsen and Dahn.[14] The x-ray-diffraction study was performed by using a Rigaku D/max-RB in the θ-2θ scan mode from 10° to 70°. Transmission electron microscopy was carried out on a JEM-200CX operating at a voltage of 200 kV. The specific heat was measured on a Quantum Design physical properties measurement system by using the thermal relaxation method. The sample, about 30 mg in weight, was thermally anchored to the sample holder, and the temperature dependence of heat capacity of the sample holder and the thermometer on it are carefully calibrated. The error of the specific-heat measurement is within 1%. The electrical resistivity was measured by using the four-probe method and gold as the electrical contact. The dc and ac susceptibilities, magnetization, and magnetic relaxation were measured by using a Quantum Design magnetic

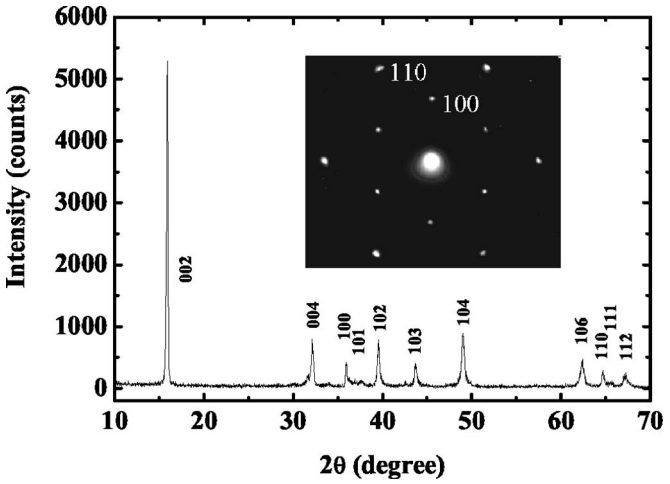

FIG. 1. X-ray diffraction of the $Na_{0.70}MnO_2$ sample at room temperature. The inset shows the electron-diffraction pattern taken along the [001] zone-axis direction.

properties measurement system. The sample (about 50 mg in weight) was mounted in a plastic capillary, and the magnetic field was parallel to the sample surface.

RESULTS AND DISCUSSIONS

Figure 1 shows the x-ray-diffraction pattern of $Na_{0.70}MnO_2$, indicating a single phase of hexagonal structure. The lattice constants can be calculated: $a=2.881$ Å and $c=11.118$ Å. The inset of Fig. 1 displays the electron-diffraction patterns for $Na_{0.70}MnO_2$ taken along the [001] zone-axis direction. All diffraction spots with strong intensity can be well indexed by a hexagonal unit cell. In contrast to the sodium ordering in $Na_{0.70}CoO_2$,[7] no diffraction spots related to Na ions vacancy superlattices have been observed. The lattice constants calculated from electron diffractions are consistent with that from x-ray diffraction within the experimental error of 2%. The electrical resistivity is characterized above 240 K, and no apparent magnetoresistance is observed at 5 T. The resistivity below 240 K is so large that it exceeds the limit of our experimental apparatus.

Figure 2(a) displays the zero-field-cooled (ZFC) and field-cooled (FC) magnetic susceptibilities of $Na_{0.70}MnO_2$ measured at $H=25$ Oe. The ZFC and FC susceptibility curves start to divaricate below 50 K. The splitting of a ZFC and FC susceptibility at low temperatures could be a hallmark of a spin-glass (SG) transition.[18,19] A peak of the ZFC susceptibility is exhibited at $T_f \approx 34$ K. The inverse ZFC susceptibility is displayed in the inset of Fig. 2(a), including a Curie-Weiss law $\chi=C/(T-\theta_W)$ fitting to the data above 150 K. An effective magnetic moment is determined to be 4.77 μ_B per Mn ion from the Curie constant C, so the Mn ions are considered to be a mixture of Mn^{3+} ($S=2$, $\mu=4.90$ μ_B) and Mn^{4+} ($S=3/2$, $\mu=3.87$ μ_B). The Weiss temperature is found to be $\theta_W=-411$ K, exhibiting an antiferromagnetic coupling between Mn ions. Due to the inability to settle each pair of Mn ions antiparallel on an equilateral triangle, the triangular network of antiferromagnetically

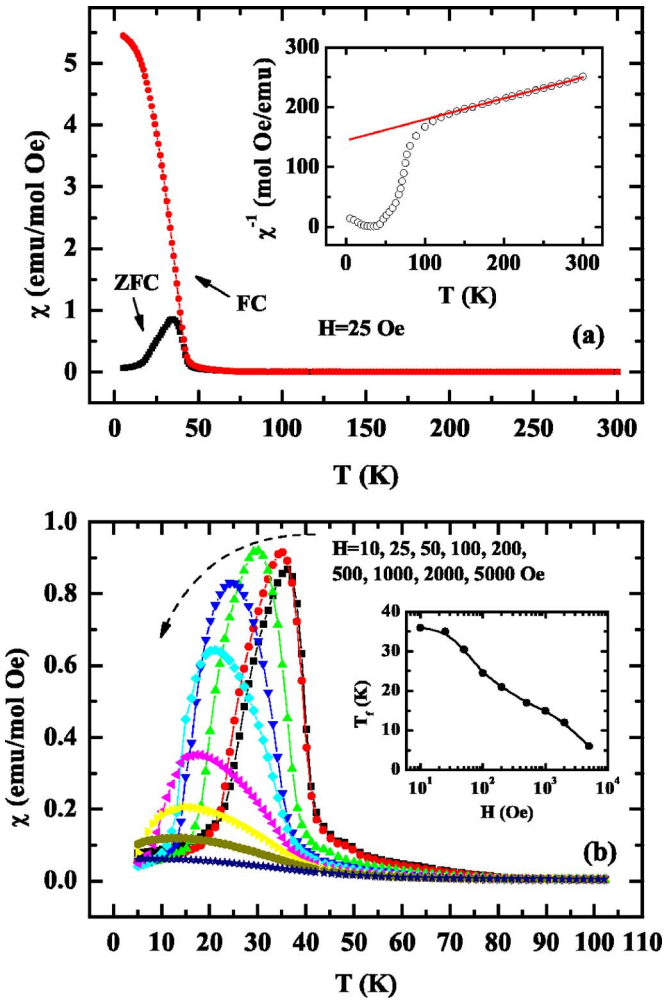

FIG. 2. (Color online) dc magnetic susceptibility $\chi(T)$ in $Na_{0.70}MnO_2$. (a) ZFC and FC susceptibility curves measured at $H=25$ Oe. The inset shows the inverse ZFC susceptibility $\chi^{-1}(T)$ with a Curie-Weiss law fit above 150 K. (b) ZFC susceptibility $\chi(T)$ measured at various magnetic fields, and the field dependence of the peak position T_f is plotted in the inset.

coupled Mn ions tends to display geometrical frustration. The degree of frustration can be measured by the ratio $f=|\theta_W|/T_f^2$, as θ_W and T_f are related to the antiferromagnetic coupling in the paramagnetic state and energy barrier height in the freezing state. The frustration degree parameter is evaluated as $f=12.1$, consistent with the presence of strong frustration. Figure 2(b) shows the ZFC susceptibility measured at various magnetic fields. Each ZFC susceptibility curve exhibits a peak, which becomes broader and shifts to lower temperatures with increasing magnetic fields. So, higher magnetic fields suppress the energy barriers and thus reduce the freezing temperature, consistent with a spin-glass transition.

Spin-glass behavior is usually characterized by the ac susceptibility, and the freezing temperature is accurately determined by the position of the cusp of the real part of the ac susceptibility χ'. Figure 3 shows $\chi'(T,\omega)$ measured with a driving field of 3.5 Oe. Below the freezing temperature $T_f=39$ K, the amplitude of χ' highly depends on the measuring

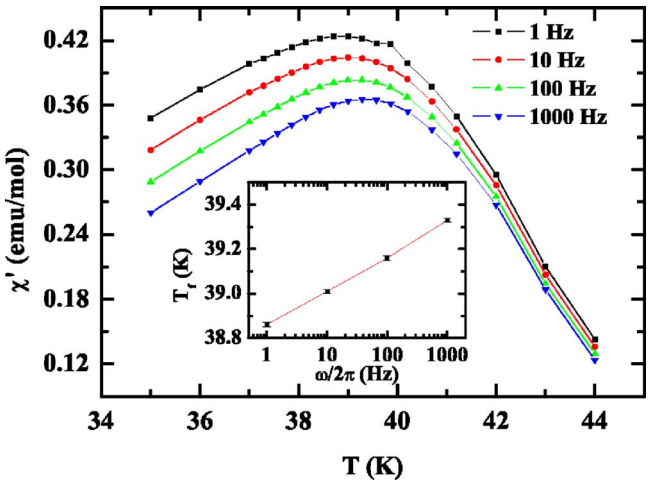

FIG. 3. (Color online) Temperature dependence of the real part of the ac magnetic susceptibility χ' measured at $\omega/2\pi=1$, 10, 100, and 1000 Hz, respectively, with a driving field of 3.5 Oe. The inset shows the frequency dependence of the peak position plotted as T_f vs $\omega/2\pi$.

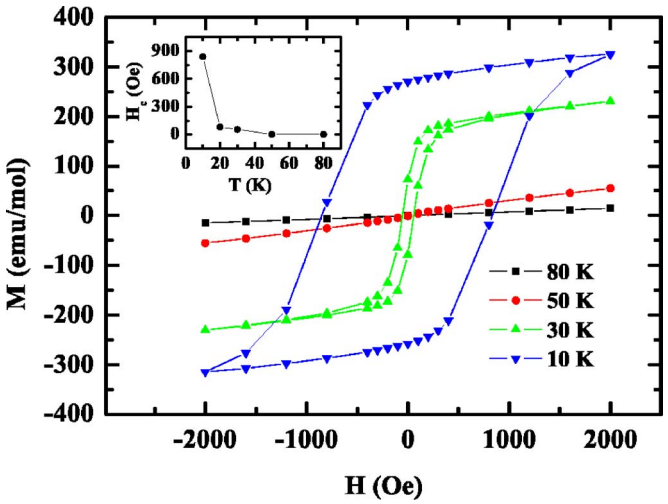

FIG. 4. (Color online) Magnetization as a function of the external magnetic field at $T=80$, 50, 30, and 10 K. The inset shows the temperature dependence of the coercive field.

frequency $\omega/2\pi$. Importantly, the peak of ac susceptibility shifts to lower temperatures with decreasing measuring frequency. Such a frequency shift is not expected for the usual antiferromagnetic or ferromagnetic long-range-ordered system.[20] Moreover, the frequency shift K defined by

$$K = \frac{1}{T_f} \frac{\Delta T_f}{\Delta \log \omega} \tag{1}$$

is calculated as 0.004, which is in the range of conventional spin-glass systems such as AuMn ($K=0.0045$) and CuMn ($K=0.005$), but much smaller than that of typical superparamagnet a-$Ho_2O_3(B_2O_3)$ ($K=0.28$).[19] The K value offers an experimental criterion to exclude the superparamagnetism from the $Na_{0.70}MnO_2$ compound and favors the spin-glass behavior.[19] In fact, the Mn ions are strongly interacting on the triangular lattice, and the concept of independent superparamagnetic particles does not apply in this compound.

To further characterize the magnetic properties of $Na_{0.70}MnO_2$ at low temperatures, we have measured the magnetic-field dependence of magnetization $M(H)$ (Fig. 4) and long-time magnetization relaxation $M(t)$ (Fig. 5). The $M(H)$ curve departs from linear relation at 50 K, and hysteresis effect is significant at lower temperatures. The coercive field $H_c(T)$ is about several decades of oersteds from 30 to 20 K, which is comparable to that observed in conventional spin-glass systems.[19] The increase of the coercive field at 10 K is due to the high freezing degree together with the small thermal activation energy. The zero-field-cooled magnetization relaxation is measured at different temperatures with a fixed measuring field of 200 Oe. However, the magnetization $M(t)$ does not display any sign of saturation even after 5000 s below 30 K, indicating that the system is far from the equilibrium. It is generally believed that the long-time magnetization relaxation should be attributed to the glassy compound when the field is larger than the coercive field.[18,21] Since the coercive fields at 25 and 20 K are sufficiently smaller than 200 Oe, the relaxation of $M(t)$ should result from glassy processes. When the coercive field is comparable to the measuring field, a much larger part of the system contributes to the magnetization relaxations (at 15 K). To check whether there are any general parameters describing the spin dynamics in the magnetization relaxation, we fit our data with the standard stretched exponential function

$$M(t) = M_0 - M_r \exp\left[-\left(\frac{t}{\tau_r}\right)^{1-n}\right], \tag{2}$$

where M_0, M_r, τ_r, and n are the ferromagnetic component, the glassy component, the relaxation characteristic time, the critical exponent, respectively. The fitting parameters are listed in Table I. The critical exponent n ($\simeq 0.5$) does not

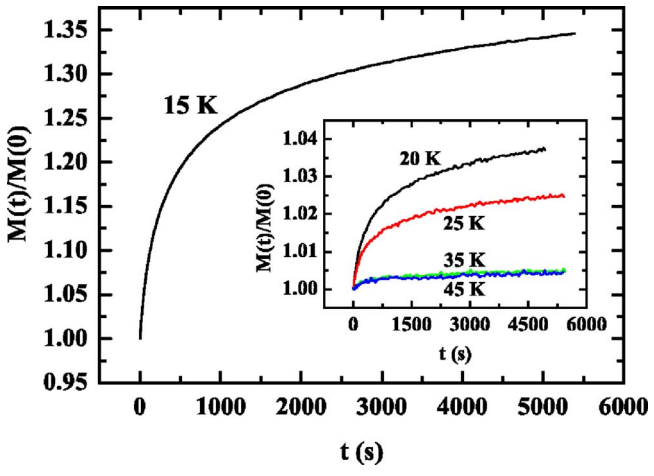

FIG. 5. (Color online) Time dependence of normalized magnetization $M(t)/M(0)$ at different fixed temperatures. In each measurement, the sample was first cooled under zero field from 200 K, and then a field of 250 Oe was applied. The time at which the field was stable is set as the initial time $t=0$.

TABLE I. Fitting parameters of the magnetization $M(t)$ with the stretched exponential function.

T (K)	M_0 (emu/mol)	M_r (emu/mol)	τ_r (s)	n
25	144.6	4.2	988	0.504±0.015
20	146.4	6.4	1097	0.498±0.011
15	126.8	37.0	792	0.508±0.008

vary with temperature, and it is the interaction strength between the local magnetic moments that governs the dynamic processes. It is noted that the value of τ_r is very sensitive to the experimental conditions [as indicated by the thermoremanent magnetization (TRM) results below], so the temperature variations of τ_r cannot be concluded from the present results.

A crucial feature of the spin-glass behavior is the existence of extremely slow spin relaxation, and this dynamics process is frequently studied by the TRM measurements.[21] The magnetization decay strongly depends on the waiting time (t_w) at a particular temperature before a sudden change of the magnetic field, i.e., the aging effect. In each measurement, the $Na_{0.70}MnO_2$ sample is cooled from the paramagnetic state with a magnetic field H_{cooled}. After being kept at 20 K for a waiting time t_w, the magnetic field is removed and the decay of magnetization $M(t)$ is measured. The magnetization decays at $H_{cooled}=10$ Oe are displayed in Fig. 6(a), and the fit with a stretched exponential function is presented in Table II. We found that the relaxation characteristic time τ_r is dependent on the waiting time (t_w). In fact, the spin relaxation in the spin-glass state has a wide relaxation-time spectrum $g_{t_w}(\tau)$,[21,22] instead of a single characteristic response time τ_r. The magnetization decay can be described as

$$M_{t_w}(t) = \int_{\tau_0}^{\infty} g_{t_w}(\tau)\exp\left(-\frac{t}{\tau}\right)d\tau, \tag{3}$$

in which $\tau_0 \approx 10^{-12}$ s is a microscopic attempt time.[21,22] So, a relaxation function $S(t)=-\frac{1}{H}\frac{dM(t)}{d\log t}$ can be used to probe the distribution function $g_{t_w}(\tau)$. The relaxation function $S(t)$ [Fig. 6(b)] exhibits a broad peak at $t\approx 250$ s for $t_w=180$ s. The peak of $S(t)$ curves shifts to larger time and becomes dispersed with increasing t_w. The fact that $S(t)$ does not exhibit a peak at $t\approx t_w$ for larger t_w suggests that the dynamic process of the spin-glass state should be governed by a reduced effective waiting time λ/t_w^{μ} defined by

$$\frac{\lambda}{t_w^{\mu}} = \frac{(t+t_w)^{1-\mu}-(t_w)^{1-\mu}}{1-\mu}, \tag{4}$$

where μ is a fitting parameter.[21] Figure 7 shows that the magnetization decay can be well scaled with λ/t_{ω}^{μ}, both for $H_{cooled}=10$ Oe and $H_{cooled}=2.5$ Oe. In both cases, the value $\mu<1$ is used, related to the so-called subaging effect.[21] The scaling of the magnetization decay reveals that the spin-glass system has strong dynamic correlations among the spin degrees of freedom and cannot be regarded as a simple disorder aggregate.

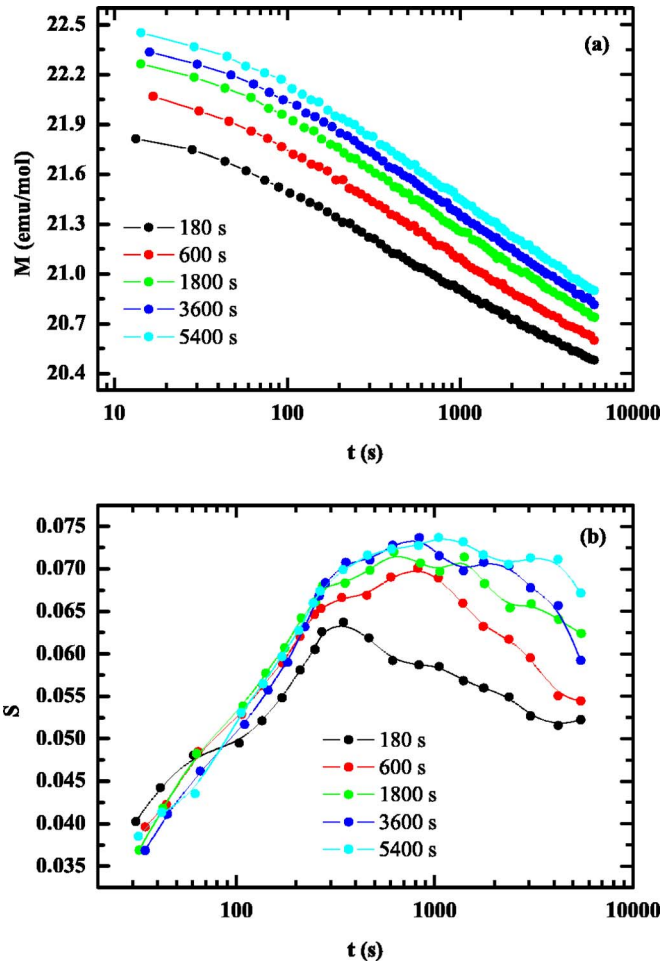

FIG. 6. (Color online) (a) Thermoremanent magnetization $M(t)$ and (b) relaxation function $S(t)$ after waiting at $T=20$ K and $H_{cooled}=10$ Oe for various times t_w.

To describe the spin-glass state theoretically, Edwards and Anderson introduced a spin-glass order parameter q as a function of temperature.[23] Based on the appropriate form of the mean-field theory, Sherrington and Kirkpatrick predicted that the spin-glass order parameter $q(T)$ vanishes at T_f as $q(T)\propto(1-T/T_f)$ below T_f.[24,25] The value of $q(T)$ can be extracted from the dc magnetic susceptibility $\chi(T)$, the Curie constant C_{SG}, and the Weiss temperature θ_{SG} as follows:[26]

TABLE II. Fitting parameters of thermoremanent magnetization (TRM) $M(t)$ after waiting various times t_w with the stretched exponential function at $T=20$ K and $H=10$ Oe.

t_w (s)	M_0 (emu/mol)	M_r (emu/mol)	τ_r (s)	n
180	20.40	−1.60	712	0.519±0.012
600	20.52	−1.74	803	0.503±0.011
1800	20.62	−1.84	903	0.511±0.012
3600	20.68	−1.85	980	0.506±0.010
5400	20.73	−1.91	1040	0.513±0.012

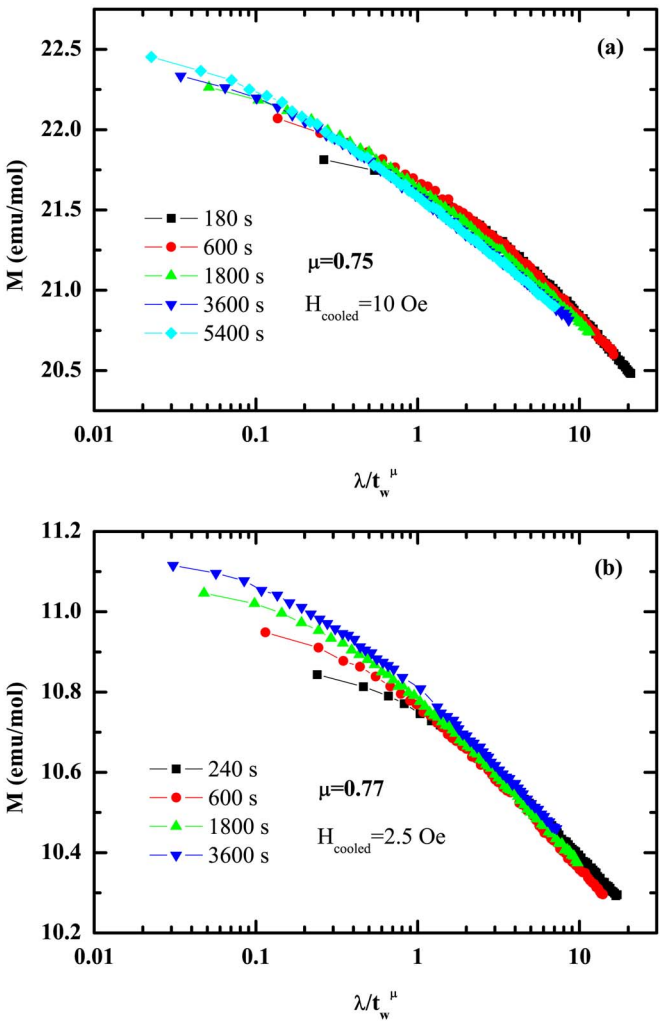

FIG. 7. (Color online) Scaling of the thermoremanent magnetization (TRM) with an effective waiting time λ/t_w^{μ} for the data measured at $T=20$ K and (a) $H_{cooled}=10$ Oe and (b) $H_{cooled}=2.5$ Oe, respectively.

$$q(T) = 1 - \frac{T\chi(T)}{C_{SG} + \theta_{SG}\chi(T)}. \tag{5}$$

The Curie constant ($C_{SG}=0.651$ emu K/mol Oe) and the Weiss temperature ($\theta_{SG}=38.4$ K) have been obtained by fitting the susceptibility with the Curie-Weiss law from 46 to 60 K. Figure 8 displays the temperature dependence of the spin-glass order parameter $q(T)$. It can be seen that $q(T)$ drops to zero at T_f. In the present compound, $Na_{0.70}MnO_2$, the order parameter exhibits the relation $q(T) \propto (1-T/T_f)^{\beta}$ (the lower inset of Fig. 8), with the critical exponent $\beta = 1.01 \pm 0.01$. This result is in good agreement with the prediction of the mean-field theory ($\beta=1$).[24] Based on the mean-field model of Sherrington and Kirkpatrick, de Almeida and Thouless (AT) studied the spin-glass state in finite magnetic fields and obtained a H-T phase diagram of the spin-glass system.[27] The phase boundary between stable and unstable states is called the AT line, which has the form $T_f \propto H^{2/3}$.[27,28] In the present compound, $Na_{0.70}MnO_2$, the field

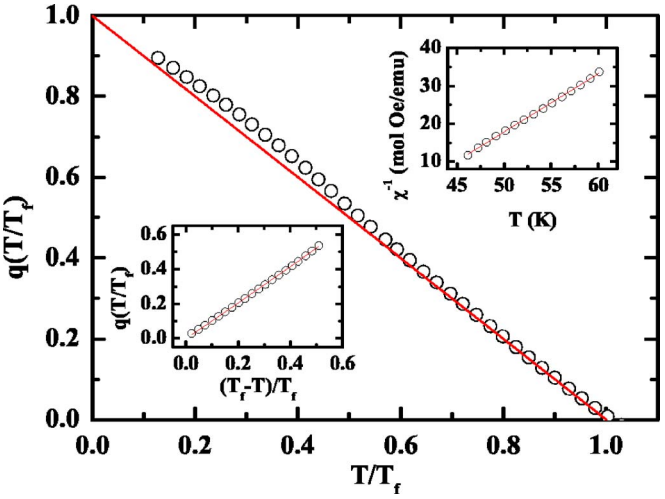

FIG. 8. (Color online) Spin-glass order parameter $q(T)$ as a function of the reduced temperature T/T_f. The solid line indicates the mean-field theory prediction. The upper inset shows the inverse ZFC susceptibility with a Curie-Weiss law fit above T_f. The lower inset displays the fitting of $q(T)$ with $q(T)=\alpha(1-T/T_f)^{\beta}$, in which $\alpha=1.05$ and $\beta=1.01$.

dependence of $T_f(H)$ [displayed in the inset of Fig. 2(b)] does not follow the AT line. However, we should mention that it is hard to define a dividing line between the stable and unstable states at finite magnetic fields. For example, the long-time relaxation can be presented even above $T_f(H)$ for a large field (such as $T=25$ K with $H=200$ Oe). Moreover, the peaks of ZFC susceptibility curves at large fields are rather broad, and the $T_f(H)$ values are simply not well defined.[18,19] Other techniques including the ac susceptibility measurements with biased dc fields[29,30] are under consideration for the further study of the field effect in this compound.

Figure 9 shows the results of specific-heat measurement for $Na_{0.70}MnO_2$. Generally, the measured specific heat (C_t) in $Na_{0.70}MnO_2$ includes the contributions from both the lattice specific heat (C_l) and the magnetic specific heat (C_m). However, in the high-temperature paramagnetic state, C_l is dominating. To estimate the magnetic specific heat (C_m), we first determine the Debye temperature, and then subtract the lattice contribution. The Debye temperature θ_D of $Na_{0.70}MnO_2$ is determined by fitting C_t above 160 K with the Debye specific-heat expression $C_V(T)=3Nk_Bf_D(\theta_D/T)$, in which $f_D(y)=\frac{3}{y^3}\int_0^y \frac{x^4e^x}{(e^x-1)^2}dx$ and $N=3.7$ is the number of atoms per unit. The Debye temperature is thus obtained: $\theta_D=578$ K. We found a broad peak in the magnetic specific heat C_m, which is typically observed in the spin glass above the freezing temperature T_f.[18] Below T_f, the magnetic specific heat behaves as $C_m=aT^{1.5}$, where a is a fitting parameter. It is noted that though $C_m \propto T$ is expected as a low-temperature signature of a spin glass,[19] a $T^{1.5}$ dependence of C_m has also been observed in some of the diluted magnetic alloys regarded as canonical spin-glass systems.[31] Moreover, in the geometrically frustrated compound $Yb_2Mn_2O_7$ with spin-glass behavior, the $T^{1.5}$ behavior of C_m is attributed to spin-wave-like excitations in the intermediate range.[32] In the present compound, $Na_{0.70}MnO_2$, the magnetic specific heat

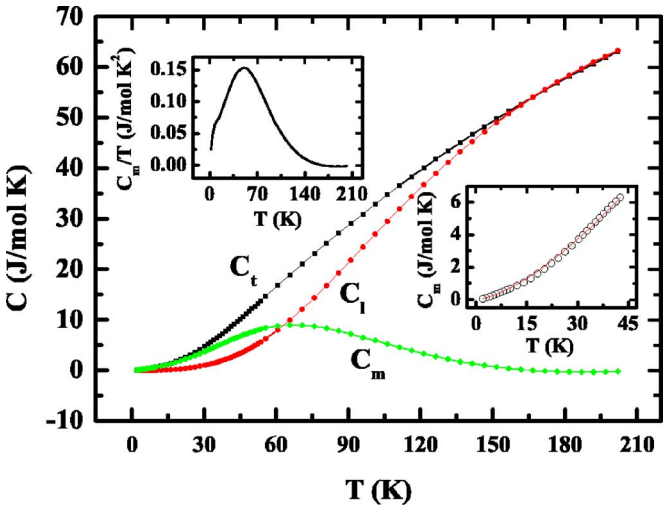

FIG. 9. (Color online) Temperature dependence of the specific heat in $Na_{0.70}MnO_2$. C_t, C_l, and C_m represent the measured total specific heat, the calculated lattice specific heat with Debye temperature θ_D=578 K, and the estimated magnetic specific heat, respectively. The upper inset shows the magnetic specific heat plotted as C_m/T vs T. The lower inset shows the fitting of $C_m=aT^{1.5}$ below T_f.

C_m expands to the temperatures above T_f, indicating that short-range ferromagnetic order is well developed before the spin-glass transition. The $T^{1.5}$ behavior of C_m may result from the spin-wave excitations of the local ferromagnetic compound, and further investigations such as neutron-diffraction experiments are suggested to clarify the results (as in the $Yb_2Mn_2O_7$ experiment[32]). To obtain the freezing degree of the $Na_{0.70}MnO_2$ compound at the lowest temperature, we calculated the magnetic entropy by integrating C_m/T from 2 to 150 K. The calculated magnetic entropy is 12.2 J/K mol. The maximum entropy for a system with 100% freezing spins is $R\ln(2S+1)$. For $S=2$ and $S=3/2$, the expected values are 11.5 and 13.4 J/K mol, respectively. Considering Mn ions as a mixture of Mn^{3+} ($S=2$) and Mn^{4+} ($S=3/2$), the magnetic moments in $Na_{0.70}MnO_2$ are almost frozen at $T=2$ K.

It can be concluded from the above experimental results that the hexagonal $Na_{0.70}MnO_2$ exhibits canonical spin-glass behavior at low temperatures. The ac susceptibility cusp at T_f=39 K and frequency-dependent susceptibility have been observed. The ZFC and FC susceptibility curves diverge below T_f, with magnetic hysteresis feature of a spin glass. The magnetic relaxation reveals that this system is metastable below T_f. To achieve a further understanding of $Na_{0.70}MnO_2$, we have to find the origin of spin-glass behavior. In the hexagonal $Na_{0.70}MnO_2$, the crystal structure consists of Mn-O layers and sodium ions between them. The spins of Mn ions within Mn-O plane form a triangular network, which is expected to cause magnetic frustrations. The ratio $f=|\theta_W|/T_f$ calculated from susceptibility measurements supports the presence of strong spin frustrations. Beyond the dominant antiferromagnetic coupling, short-range ferromagnetic order is well developed at low temperatures, indicated by the magnetic specific heat C_m and the positive Weiss temperature around T_f (θ_{SG}=38.4 K). The competitions of antiferromagnetic and ferromagnetic coupling are expected to cause magnetic instability, and the exact spin configurations in the ground state are very sensitive to the experimental conditions. Microscopically, the $Mn^{3+/4+}$-$Mn^{3+/4+}$ direct interaction is in antiferromagnetic coupling, while the $Mn^{3+/4+}$-O-$Mn^{3+/4+}$ superexchange is in ferromagnetic coupling, according to Goodenough.[33] In the present compound, $Na_{0.70}MnO_2$, Mn ions are considered as a mixture of Mn^{3+} ($S=2$) and Mn^{4+} ($S=3/2$) ions. The distributions of Mn^{3+}/Mn^{4+} are influenced by Na^+ ions, and no sign of electron-diffraction spots related to Na^+ ion ordering has been observed. So, the Mn^{3+}/Mn^{4+} mixture is expected to distribute on the triangular lattice randomly. Based on this argument, geometrical frustration and Mn^{3+}/Mn^{4+} mixture are likely to play a crucial role in the formation of the spin-glass state.

Finally, we compare the magnetic properties of $Na_{0.70}MnO_2$ with that of $Na_{0.70}CoO_2$. According to the previous reports, $Na_{0.70}CoO_2$ exhibits the Curie-Weiss form susceptibility $\chi-\chi_0=C/(T-\theta_W)$, with $\theta_W\approx-100$ K.[11,12,34] Since θ_W is determined by the antiferromagnetic coupling strength of the magnetic ions, the results suggest that the antiferromagnetic coupling is stronger in $Na_{0.70}MnO_2$ (θ_W =−411 K) than that in $Na_{0.70}CoO_2$. The mobility of Na^+ ions in $Na_{0.70}CoO_2$ is so large that they tend to form well ordered superstructure, which is shown by the electron diffractions[7] and NMR experiments.[11] In contrast to the spin-glass transition at 39 K in $Na_{0.70}MnO_2$, $\chi(T)$ of $Na_{0.70}CoO_2$ increases rapidly at low temperatures, and no magnetic transition occurs down to 1.5 K.[11] It is noticeable that the susceptibility[12,35] $\chi(T)$ and thermopower[5] of $Na_{0.70}CoO_2$ have strong field dependences due to the suppressions of spin fluctuations and spin degrees of freedom by magnetic field. Thus, geometrical frustrations induce a magnetic instability in $Na_{0.70}CoO_2$, and such a magnetic instability coupled with the high-mobility carriers is expected to play a key role in the formation of complex phase diagram. However, the electrical resistivity in $Na_{0.70}MnO_2$ is so large that the low-temperature electronic properties are hard to be detected. If the carrier density is increased to make Na_xMnO_2 become metallic, the coupling of electronic and magnetic frustrations may also emerge in this system. The related studies[36] indicated that the electrical conductivity of $Na_{0.70}MnO_2$ can be changed remarkably by removing some sodium ions, revealing the possibility of controlling the physical properties of Na_xMnO_2 by adjusting the amount of sodium ions in the structure. Further electronic experiments on Na_xMnO_2 are needed to understand the complex ground state of triangular lattice antiferromagnets.

In conclusion, we have studied the magnetic and thermodynamic properties of the hexagonal insulating compound $Na_{0.70}MnO_2$. The characteristics of the canonical spin-glass transition have been observed. Irreversibility, frequency dependence of ac susceptibility, magnetic hysteresis, long-time relaxation, and cusp of the magnetic specific heat have been discussed. The spin-glass formation is ascribed to the complexity of the Mn^{3+}/Mn^{4+} mixtures with strong geometrical frustrations.

ACKNOWLEDGMENTS

We thank C. M. Xiong for helpful discussions. This work was supported by the National Science Foundation of China (Grants No. 50425205, No. 10674079, and No. 50272031), 973 project (No. 2002CB613505), Specialized Research for the Doctoral Program of Higher Education (No. 20030003088), and National Center for Nanoscience and Technology of China.

*Electronic address: ygzhao@tsinghua.edu.cn

[1] M. F. Collins and O. A. Petrenko, Can. J. Phys. **75**, 605 (1997).
[2] J. E. Greedan, J. Mater. Chem. **11**, 37 (2001).
[3] K. Takada, H. Sakural, E. Takayama-Muromachi, F. Izumi, R. A. Dilanian, and T. Sasaki, Nature (London) **422**, 53 (2003).
[4] I. Terasaki, Y. Sasago, and K. Uchinokura, Phys. Rev. B **56**, R12685 (1997).
[5] Y. Y. Wang, N. S. Rogado, R. J. Cava, and N. P. Ong, Nature (London) **423**, 425 (2003).
[6] M. L. Foo, Y. Wang, S. Watauchi, H. W. Zandbergen, T. He, R. J. Cava, and N. P. Ong, Phys. Rev. Lett. **92**, 247001 (2004).
[7] H. W. Zandbergen, M. L. Foo, Q. Xu, V. Kumar, and R. J. Cava, Phys. Rev. B **70**, 024101 (2004).
[8] S. Y. Li, L. Taillefer, D. G. Hawthorn, M. A. Tanatar, J. Paglione, M. Sutherland, R. W. Hill, C. H. Wang, and X. H. Chen, Phys. Rev. Lett. **93**, 056401 (2004).
[9] L. M. Helme, A. T. Boothroyd, R. Coldea, D. Prabhakaran, D. A. Tennant, A. Hiess, and J. Kulda, Phys. Rev. Lett. **94**, 157206 (2005).
[10] A. T. Boothroyd, R. Coldea, D. A. Tennant, D. Prabhakaran, L. M. Helme, and C. D. Frost, Phys. Rev. Lett. **92**, 197201 (2004).
[11] I. R. Mukhamedshin, H. Alloul, G. Collin, and N. Blanchard, Phys. Rev. Lett. **93**, 167601 (2004).
[12] L. B. Luo, Y. G. Zhao, G. M. Zhang, S. M. Guo, L. Cui, and J. L. Luo, Phys. Rev. B **73**, 245113 (2006).
[13] J. P. Parant, R. Olazcuaga, M. Devalette, C. Fouassier, and P. Hagenmuler, J. Solid State Chem. **3**, 1 (1971).
[14] J. M. Paulsen and J. R. Dahn, Solid State Ionics **126**, 3 (1999).
[15] P. J. Baker, T. Lancaster, S. J. Blundell, M. L. Brooks, W. Hayes, D. Prabhakaran, and F. L. Pratt, Phys. Rev. B **72**, 104414 (2005).
[16] S. de Brion, C. Darie, M. Holzapfel, D. Talbayev, L. Mihály, F. Simon, A. Jánossy, and G. Chouteau, cond-mat/0608238 (unpublished).
[17] A. Olariu, P. Mendels, F. Bert, B. G. Ueland, P. Schiffer, R. F. Berger, and R. J. Cava, Phys. Rev. Lett. **97**, 167203 (2006).
[18] K. Binder and A. P. Young, Rev. Mod. Phys. **58**, 801 (1986).
[19] J. A. Mydosh, *Spin Glass: An Experimental Introduction* (Taylor & Francis, London, 1993).
[20] J. A. Mydosh, J. Magn. Magn. Mater. **158**, 606 (1996).
[21] E. Vincent, J. Hammann, M. Ocio, J. P. Bouchaud, and L. F. Cugliandolo, cond-mat/9607224 (unpublished).
[22] L. Lundgren, P. Svedlindh, P. Nordblad, and O. Beckman, Phys. Rev. Lett. **51**, 911 (1983).
[23] S. F. Edwards and P. W. Anderson, J. Phys. F: Met. Phys. **5**, 965 (1975).
[24] D. Sherrington and S. Kirkpatrick, Phys. Rev. Lett. **35**, 1972 (1975).
[25] S. Kirkpatrick and D. Sherrington, Phys. Rev. B **17**, 4384 (1978).
[26] T. Mizoguchi, T. R. McGuire, S. Kirkpatrick, and J. R. Gambino, Phys. Rev. Lett. **38**, 89 (1977).
[27] J. R. L. de Almeida and D. J. Thouless, J. Phys. A **11**, 983 (1978).
[28] H. A. Katori and A. Ito, J. Phys. Soc. Jpn. **63**, 3122 (1994).
[29] J. Mattsson, T. Jönsson, P. Nordblad, H. Aruga Katori, and A. Ito, Phys. Rev. Lett. **74**, 4305 (1995).
[30] P. E. Jönsson, H. Takayama, H. A. Katori, and A. Ito, Phys. Rev. B **71**, 180412(R) (2005).
[31] J. O. Thomson and J. R. Thomson, J. Phys. F: Met. Phys. **11**, 247 (1981).
[32] J. E. Greedan, N. P. Raju, A. Maignan, Ch. Simon, J. S. Pedersen, A. M. Niraimathi, E. Gmelin, and M. A. Subramanian, Phys. Rev. B **54**, 7189 (1996).
[33] J. B. Goodenough, *Magnetism and the Chemical Bond* (Wiley, New York, 1963).
[34] J. L. Gavilano, D. Rau, B. Pedrini, J. Hinderer, H. R. Ott, S. M. Kazakov, and J. Karpinski, Phys. Rev. B **69**, 100404(R) (2004).
[35] F. Rivadulla, M. Banobre-Lopez, M. Garcia-Hernandez, M. A. Lopez-Quintela, and J. Rivas, Phys. Rev. B **73**, 054503 (2006).
[36] S. Hirano, R. Narita, and S. Naka, Mater. Res. Bull. **19**, 1229 (1984).